



Hybrid Optimization with Enhanced QoS-based Path Selection in VANETs

F. Al-dolaimy¹ Rabei Raad Ali^{2*} Noor Nabeel³ Wisam Subhi Al-Dayeni⁴
 Fatima Hashim Abbas⁵ Hussein Muhi Hariz⁶ Salama A Mostafa⁷
 Mohammed Ahmed Jubair⁸

¹Al-Zahraa University for Women, Karbala, Iraq

²Department of Computer Engineering Technology, Northern Technical University, 41001, Mosul, Iraq

³Northern Technical University, Administrative Technical College, 41001, Mosul, Iraq

⁴School of Information Technologies and Engineering, ADA University, Baku, Azerbaijan, AZ1008

⁵Medical Laboratories Techniques Department, Al-Mustaqbal University College, 51001 Hillah, Babil, Iraq,

⁶Department of Computer Techniques Engineering, Mazaya University College, 6400, DhiQar, Iraq,

⁷Faculty of Computer Science and Information Technology,
 Universiti Tun Hussein Onn Malaysia, 86400, Johor, Malaysia

⁸Department of Computer Technical engineering, College of Information Technology
 Imam Ja'afar Al-Sadiq University, 66001, Al-Muthanna, Iraq,

* Corresponding author's Email: rabei@ntu.edu.iq

Abstract: Vehicular ad hoc networks (VANETs) recently covered a wide range of intelligent transportation systems (ITSs) and applications. VANETs consist of convinced unique characteristics such as dynamic movement and high speed. Due to these characteristics, link failures occur, and delay and routing overhead is greatly increased, directly affecting the effectiveness, Quality of Service (QoS), and stability of VANETs. To achieve an efficient and reliable network performance, this paper proposes QoS Aware Hybrid Optimization for Improving Path Selection (HOIPS-VANETs) in VANETs. This hybrid optimization combines the Improved ant colony optimization (ACO) and Effective Whale Optimization Algorithm (EWOA). The EWOA algorithm is used for initial optimal path selection, and ACO is used to find the best optimal solution to achieve effective communication in VANETs. This optimization technique is also applied to low-density, medium-density, and high-density scenarios, as it is compared with the earlier methods. During the experimentation process, our findings reveal no noticeable change in the performance of the earlier methods when applied to the low-density and medium-density scenarios. Still, the performance is gradually reduced when applied to the high-density scenario. On the other hand, the performance of the proposed approach is better for all three tested scenarios and demonstrates effective communication for the VANETs.

Keywords: Vehicular ad hoc networks, Intelligent transportation systems, Quality of service, Hybrid optimization, Improved ant algorithm, Effective whale optimization algorithm.

1. Introduction

Vehicular Ad-hoc network (VANETs) have certain special characteristics, such as high dynamic mobility, high-speed vehicles, and complex vehicle distribution. It has been adapted in intelligent transportation systems (ITS). These features cause high path loss, link failure, and delay. Due to this drawback, the efficiency, packet delivery ratio, and network throughput are highly affected [1, 2]. It is

essential to secure vehicles from serious issues like road accidents and traffic congestion.

VANETs communication is performed using the dedicated short-range communication (DSRC) protocol. The physical/MAC layers are constructed using the wireless access in vehicular environment protocol. Through VANETs, real-time wireless data exchange is performed; therefore, significant safety benefits are highly concentrated. The communication

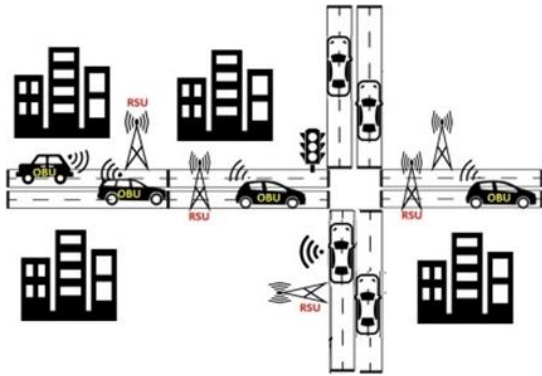


Figure. 1 VANETs communication [3]

modules of VANETs consist of vehicle communication and vehicle to infrastructure communication [3]. To achieve effective communication in VANETs, finding the optimal best path between the sending and receiving vehicles is essential. It may also include other devices like neighbour vehicles and Roadside Units (RSU). Fig. 1 shows the architecture of VANETs' communication.

Reliable data transmission can be attained by ensuring the best quality of service (QoS) with low delay and routing overhead. The matter of optimum route selection can achieve it. Hence the vehicles in VANETs are highly movable. Frequent topology changes will occur in the network, which leads to high delay and packet loss during communication [4, 5]. A maximum delay occurs during the transmission between the vehicles and the RSUs. So, deploying sufficient RSUs on the roadside is essential to achieve minimum delay cost-effectively. In earlier research, several methods are introduced to achieve this target which is heuristic and meta-heuristic algorithms to solve the set-covering and greed set cover" problems [6]. The particle swarm optimization approach is developed to increase the convergence speed of the network so that effective communication can be achieved in vehicle to infrastructure communication [7, 8]. Research optimization is concentrated on monitoring the network traffic and best path selection to improve the capacity of the VANETs network. But currently, the number of vehicles utilized in a real-time environment is highly increased, so achieving the shortest path from the source to the destination is still an open research area. To attain maximum reliability in multi-hop VANETs, all the parameters must be properly identified to accomplish cooperative communications. For that purpose, in our paper,

- QoS aware hybrid optimization for improved path selection (HOIPS-VANETs) is proposed.
- HOIPS-VANETs combines highly effective optimization algorithms such as ACO and

effective whale optimization algorithm (EWOA).

- Finally, a developed simulation for testing and evaluating the HOIPS-VANETs method.

The following section of this paper presents a summary of the related work. Sections III and VI present the contributions of the paper. Section V presents the performance analysis. VI presents the results and discussion. Section VII presents the conclusion and lists the possible future work.

2. Related works

In [9], show how to maximize the coverage ratio in a VANET using improved particle swarm optimization (IPSO), which was motivated by the food-finding behaviour of bird or fish swarms. To offer the isolated cars the best connectivity possible, internet of drone nodes were deployed according to the positions of the vehicles at any given time. The stable connection and coverage maximization are its key benefits. However, this method produces high latency. In [10], introduce two discrete versions of the cuckoo search optimization (CSO) technique: The Lévy light-based discrete CSO (LF-DCSO) and the random walk-based discrete CSO (RW-DCSO) for efficient route discovery on VANETs. The advantage is that it improves communication link dependability. When the service area expands, though, this causes the network to become more complicated.

In [11], develop ant colony-based temporarily ordered algorithm to provide the shortest routes based on vehicle priority. This framework achieves an enhanced packet delivery rate with minimized packet loss, average cluster duration, and low energy consumption. But the major drawback of this framework is the traffic congestion level cannot be reduced if the motorist disregards the route recommendation. In [12], create an analytical deployment framework for deploying BSs and energy harvest roadside units in specific low-frequency service zones to lower the cost of deployment and maintenance in VANET. To minimize deployment and operating expenses, an optimization issue is put forth. This framework's key benefit is considerably lowering operations and deployment costs, but it needs to expand network communication flexibility or reduce network overhead.

In [13], introduce the "Greedy3P4" greedy method for the RSU deployment. This framework's primary benefit is that it is appropriate for real-time implementation. This approach enables higher PDR

Table 1. Definition of terms

| notation | meaning |
|----------------------------|--------------------------------|
| Horizontal position | $x_i(t_0)$ |
| Position of vehicle | $x_i(t_0 + \Delta t_0)$ |
| Speed of vehicle | $v_i(t_0 + \Delta t_0)$ |
| Horizontal distance | $\Delta T_i(t_0 + \Delta t_0)$ |
| Minimum values | v_{min} |
| Maximum values | v_{max} |
| Number of packet exchanges | NoPE |
| Global pheromone | τ_G |
| Vehicles at the hop | VA_i |
| Coefficient vectors | $\vec{C}_1 \vec{C}_2$ |
| Random vector | \vec{r}_1 |
| Iteration number | t_0 |
| Position vector | \vec{Y} |
| Number of CHs. | K |

and lower energy usage even in crowded network environments. However, only road crossings were considered as candidate places to make the challenge less challenging, which obviously decreased the quality of the responses. In [14], present an efficient and collaborative framework. This framework provides a quicker detection time, a greater detection rate, and less overhead using Markov-based reputation scheme. However, this framework's primary flaw is that it is unsuitable for real-time applications because of its higher network delay and decreased dependability.

3. System model

VANET technology has undergone numerous changes and advancements [15-21]. There will be data traffic in the network transmission route when there are many vehicles. This is the primary problem examined, and a better path selection is needed to improve data flow. The positioning of a vehicle, which serves as a neighbour node, can affect the performance of information distribution. The intersection connectivity is generally enhanced via RSU placement. The proposed approach uses reports from vehicles inside the RSU communication range to determine the ideal place for RSU. The RSU installation is suggested to expand the number of connected vehicles. However, the communication between vehicles and infrastructure (V2I) is restricted by the physical obstructions between the receiver and the transmitter, limiting the broadcast signal. Table 1 shows all the notations that are being used throughout this paper.

In VANETs, there is a lot of temporal and spatial connectivity between vehicles. The location history

state of a vehicle denotes its leading vehicle, which has comparable motion properties that can be used to pinpoint the position of a vehicle within a certain interval. An initial position and initial velocity are given to each vehicle. The vehicles maintain specific restrictions and motion patterns as they travel over time. The horizontal position of the i^{th} vehicle at time t_0 is denoted by $x_i(t_0)$, while its previous and subsequent vehicles are $x_{i+1}(t_0)$ and $x_{i-1}(t_0)$, accordingly.

The speedy vehicle i is between the two extremes, which is $\vartheta_i(t) \in [\vartheta_{max}, \vartheta_{min}]$ and acceleration is $a_i(t_0)$, the vehicle's present speed is defined by its starting speed and acceleration. After the time interval Δt_0 , the position of vehicle i will have changed to $x_i(t_0 + \Delta t_0)$, and its speed will increase with $v_i(t_0 + \Delta t_0)$. Thus, Eq. (1 and 2) are the calculation of the speed, and the moving behaviour of the vehicle is given in.

$$x_i(t_0 + \Delta t_0) = \left(v_i(i)\Delta t_0 + \frac{1}{2} a_i(t_0)\Delta t_0^2 \right) + x_i(t_0) \quad (1)$$

$$v_i(t_0 + \Delta t_0) = v_i(t_0) + a_i(t_0)\Delta t_0 \quad (2)$$

The horizontal distance between the i^{th} vehicle and the $(i + 1)th$ vehicle is given in Eq. (3)

$$\Delta T_i(t_0 + \Delta t_0) = x_{i+1}(t_0 + \Delta t_0) - x_i(t_0 + \Delta t_0) \quad (3)$$

The network connectivity between two vehicles is based on the most important parameters, such as distance, link duration, and stability. With considering the broadcast coverage between vehicles is r , the necessary condition for the vehicle i and vehicle $i + 1$ to have timely communication t_0 is $\Delta T_i(t) \leq r$. Also, the maintenance of the communication link needs to be guaranteed for a specific period; otherwise, connectivity failure happens. The vehicle speed is restricted to a specific range since they are typically not permitted to reverse while driving and because urban roadways will have speed limitations is given in Eq. (4)

$$\begin{cases} \text{if } (v_i(t_0) < v_{min}), & v_i(t_0) = v_{min} \\ \text{if } (v_i(t_0) > v_{max}), & v_i(t_0) = v_{max} \end{cases} \quad (4)$$

The starting vehicle speed and acceleration should be retained throughout that legal range with a random distribution between the given maximum and minimum values. The speed-acceleration equation can be used to determine the speed of a moving object

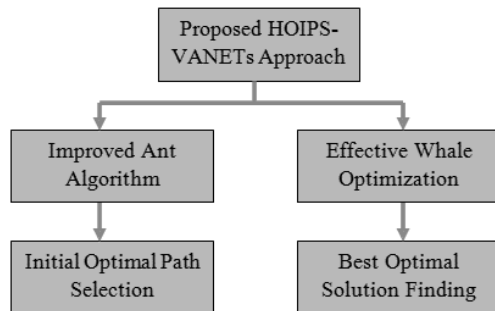


Figure. 2 The proposed HOIPS-VANETs approach

at any given time. Additionally, a safe distance is kept between each vehicle node.

4. HOIPS-VANETS approach

The HOIPS-VANETS approach combines two effective optimization algorithms such as ACO and EWOA. In our hybrid optimization process, optimization is performed on two levels: initial optimal path selection and best optimal solution finding. In the HOIPS-VANETS algorithm, ACO is used for initial optimal path selection, and the EWOA algorithm is used for the best optimal solution-finding process. The workflow of the proposed HOIPS-VANETS approach is illustrated in Fig. 2.

4.1 Improved ant colony optimization (ACO)

Ants can most effectively and intelligently find the shortest route from their colony to a food source. It is referred to as ACO and swarm intelligence-based technique that insect and animal behaviour principally inspired. Ants release chemical substances called pheromones along their path as they seek food to identify the area they have travelled. The following ants can gather information about the shortest route to food through the pheromones that have been produced. The high concentration of pheromone, which evaporates, attracts ants over time. Ants can quickly find the best way since the shortest path maintains a higher pheromone concentration than the longer path. The proposed algorithm has been designed based on the following assumptions.

- Each vehicle is equipped with a GPS and an on-board unit (OBU) module. The OBUs provide information on the vehicles, such as GPS coordinates, speed, the route toward the next vehicle, and infrastructure.
- Using a periodic beacon, vehicles broadcast their current location so that other vehicles inside the coverage area can transfer the data to the desired location.

- Buildings and other obstructions do not impact the signal propagation loss in this situation.
- When the source transmits, not all vehicles receive data packets simultaneously.

The source vehicle transmits forward ant packets to send a packet to the target vehicle. When the hop count constraint reaches the maximum set value, packets stop covering the already covered vehicle. The hop count is examined, and the pheromone trail is adjusted when the vehicle receives a forward ant transmission. The total amount of pheromones associated with the entire route is comparable to each intermediate link's unique pheromone. As soon as next hop vehicle B receives a packet from the sender, it transmits it to the next phase of vehicles, which then receives it and inform the previous phase with an acknowledgment (ACK) signal and packet recognition. Vehicles A and C do not transmit data packets to the following layer because transmitting consumes more energy than receiving. Parallel to the next layer, only the highest quality route is used for packet transmission. It cannot transmit packets to the next hop when the next hop vehicle is unavailable or challenging to reach due to a hop breakdown in the link between them. The following hop from vehicle D to vehicle F is outside of the acceptable range due to a catastrophic event or a coverage problem. After that, vehicle D utilizes V2I communication to transmit a unicast message and the packet to the closest RSU. Then, the RSU transmits the packet and builds a pseudo-ant vehicle to terminate the Data transmission. This method can manage data transmitting in both areas with heavy traffic and areas with light traffic, where an extensive number of vehicles are not present. Forward ant packets transform into backward ant packets once they arrive at their final destination. The source vehicle is visited by backward ant packets using the same procedure. The earlier route taken by the forward ant might not be exactly where the later one takes place. The reliability of the routing path is determined by the diversity of the lists of vehicles found by the leading and rear ant vehicles. To determine the precise position of the target and the present forwarder, location-based services are used. Data is transmitted to the target unless the target is outside the coverage area of the present vehicle's broadcast range. In this case, the current vehicle seeks the optimal path to transmit the data to the target. The data packet is routed if the present forwarder locates the next hop node; else, a unicast join request is transmitted to the closest RSU. The RSU developed a pseudo-ant vehicle to reach its destination. After obtaining an ant

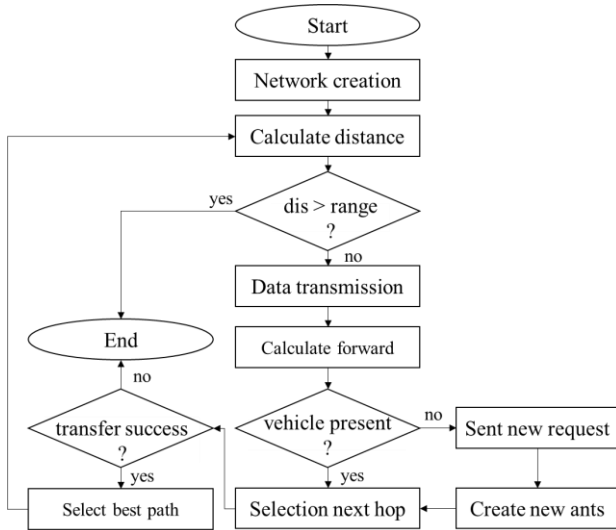


Figure. 3 Process of ACO model

packet, vehicles transmit an ACK packet. Global pheromones will be updated following a GPS distance calculation from the user's position to the destination. When the destination is reached, a transformation from forward to backward occurs, and the ant then travels back in the opposite direction to the source. When a source obtains backward ant packets, it uses the global pheromone level to find the shortest path and delivers information to the destination. The most stable path exhibits similarities between forward and backward motion. The route is followed for data transfer. The process of the ACO model is described in Fig. 3. For future ants to choose a path much more informedly, the pheromone is dispersed along the ant's travel path.

A forward ant packet converts to a backward ant only occurs when the transmission delay to the target is less than the threshold limit. Backward ants primarily determine the routing reliability. Both ant packets keep their unique ant tables to provide the optimum route while returning to the source. The vaporization level of the pheromone, as it changes over time, determines the link quality or longevity. The pheromone is applied to a specific connection. φ_{BF} is calculated by the sum of link sustainability and possibilities of getting successful packets as shown in Eq. (5).

$$\varphi_{BF} = l_{SF} + P_{pkt}^{BF} \quad (5)$$

where the term l_{SF} implies the sustainability of the link between vehicles B and F, and P_{pkt}^{BF} implies the possibilities of successful packets. The vehicle is situated in the center of the broadcast range, where link quality computation gives maximum significance to direction-matching packet flow and minimum velocity. P_{pkt}^{BF} implies the ratio between

ant packets transmitted by the previous vehicle and ant packets acquired from the next hop vehicle.

$$P_{pkt}^{BF} = \frac{P_R^F}{P_F^B} \quad (6)$$

where ant "a" is changing links from B to F. The possibility that Ant 'a' is shown in Eq. (7).

$$P_{BF}^a = \frac{[\tau_{BF}(t_0)]^\alpha [\gamma_{BF}(t_0)]^\beta}{\sum_{F \text{ allowed}} a [\tau_{BF}(t_0)]^\alpha [\gamma_{BF}(t_0)]^\beta} \quad (7)$$

where $\gamma_{BF}(t_0)$ implies the adaptive coefficient, and $\tau_{BF}(t_0)$ implies the pheromone density level. To limit the impact of $\tau_{BF}(t_0)$ and $\gamma_{BF}(t_0)$ is $0 \leq \alpha$ and $\beta \geq 1$. The mathematical expression for the calculation of $\tau_{BF}(t_0)$ is given in Eq. (8).

$$\tau_{BF} = (1 - \rho + \eta)\tau_{BF} + \rho\eta\tau_0 \quad (8)$$

where ρ is the pheromone's vaporization coefficient, η is the pheromone stability factor, τ_0 is the basic pheromone value for links B and F. The sum of each ant packet's arcs can be used to calculate the total pheromone level. Once the ant packets validate the route to choose the optimum stable path, a general updating process is carried out. The global pheromone amount for the entire path is indicated mathematically in Eq. (9).

$$\tau_G = \tau_G(1 + \eta) - \rho(\tau_G - \frac{\eta}{delay} - \eta.stabilit) \quad (9)$$

While the delay is measured by the time it takes a forward ant packet to travel from the source to a backward ant that the source has received. The degree of similarity among the forward and backward ant tables is called stability. For our suggested algorithm, the required number of packet exchanges (NoPE) is:

$$NoPE = \sum_{i=0}^n (v_i + c_i) * 2 \quad (10)$$

where v_i implies the number of vehicles transmitting packets at each hop, c_i is the package that was delivered to the additional vehicle. The ACK packets result in a doubling of the packet count. The NoPE for ACO mathematically expressed below.

$$NoPE^{IAA} = \sum_{i=0}^n (VA_i) * F_i \quad (11)$$

where VA_i implies all the vehicles at the hop, and F_i implies retry or incomplete packet transmission. Transmission failure rates increase as the number of participating automobiles increases. The fastest and most stable path is chosen as the optimum route for

data transmission since it has the most pheromones placed along it. Vehicles transmit forward after a set time if a path is not provided. According to this process, the initial path selection is performed in the network to find the optimal solution.

4.2 Effective WOA optimization

EWOA algorithm is among the simple, powerful, and swarm intelligence-based meta-heuristic techniques that utilize the intelligence of the humpback whales hunting behaviour. EWOA algorithm is highly effective in finding the global solution for the optimization problem, concentrating on all the unconstrained optimization trouble. The core principle of the EWOA is the bubble-hunting strategy that mimics the hunting characteristics of whales. The search is initiated using a random solution, the initial positions are identified with the agent's help, and the best solution is identified. The improved version of the EWOA is used in our research, called the strategy based embedded EWOA, to achieve an effective solution for the optimization problem in the VANETs network. This optimization concept includes whale initialization, exploitation, and effective exploration. Using this process, an effective best optimal solution is found during network communication. EWOA's mathematical model is divided into three phases: prey encircling, exploitation, and exploration. Prey encircling phase: EWOA starts with the encirclement of the prey (optimal agent) by humpback whales (search agents). The targeted prey is then identified as the current and best possible solution. All other search agents then make an effort to advance in the direction of the best option after the best search agent has been identified in the Eqs. (12) and (13):

$$\vec{D} = |\vec{C}_1 \cdot \vec{Y}^*(t_0) - \vec{Y}(t_0)| \quad (12)$$

$$\vec{Y}(t_0 + 1) = \vec{Y}^*(t_0) - \vec{C}_2 \cdot \vec{D} \quad (13)$$

where the terms \vec{C}_1 and \vec{C}_2 imply the coefficient vectors, and t_0 denotes the iteration number. $\vec{Y}^*(t_0)$ and \vec{Y} vectors relate to the position vector and the best agent position vector. Also, if an optimum solution can be found in each iteration, \vec{Y}^* should be enhanced. Additionally, vectors \vec{C}_1 and \vec{C}_2 are represented as follows:

$$\vec{C}_1 = 2\vec{r}_1 \quad (14)$$

$$\vec{C}_2 = 2\vec{a} \cdot \vec{r}_1 - \vec{a} \quad (15)$$

where \vec{r}_1 is a random vector in $[0, 1]$, \vec{a} is a vector that decreases linearly from 2 to 0 during the iteration process. Exploitation phase: The numerical analysis of the bubble-net attacking approach is described with these methods: Shrinking encircling approach: In this mechanism, the value of \vec{C}_2 is randomly chosen between $[-1, 1]$. Moreover, A search agent's new position could be anywhere between the current position of the agent and the position of the newest optimum agent. The spiral upgrading position approach begins with computing the distance between the agent ($\vec{Y}(t_0)$) and the optimum agent ($\vec{Y}^*(t_0)$). Then, it uses motions that mimic the spiralling motion of humpback whales (5).

$$\vec{Y}(t_0 + 1) = \vec{Dis} \cdot e^{\varphi l} \cdot \cos(2\pi l) + \vec{Y}^* \quad (16)$$

where the terms $\vec{Dis} = \vec{Y}^*(t_0) - \vec{Y}(t_0)$ imply the distance, φ implies a constant, and the value l implies a random number between $[-1, 1]$. Then, with a 50% level of probability, EWOA updates the search agent's position and chooses between the spiral mechanism and the shrinking encircling method follows:

$$\vec{Y}(t_0 + 1) = \begin{cases} \vec{Y}^*(t_0) - \vec{C}_2 \cdot \vec{D} & \text{if } p < 0.5 \\ \vec{Dis} \cdot e^{\varphi l} \cdot \cos(2\pi l) + \vec{Y}^* & \text{if } p \geq 0.5 \end{cases} \quad (17)$$

where p implies a random number between $[0; 1]$ and followed process exploration phase is initiated.

Exploration phase: The other search agents update their positions while guided by the ideal search agent chosen earlier. In addition, WOA employs \vec{C}_2 to generate a random value between -1 and 1 that allows the search agents to travel far from the benchmark agent. The following is mathematical representation of this phase is given below:

$$\vec{D} = |\vec{C}_1 \cdot \vec{Y}_{rand}(t_0) - \vec{Y}(t_0)| \quad (18)$$

$$\vec{Y}(t_0 + 1) = \vec{Y}_{rand} - \vec{C}_2 \cdot \vec{D} \quad (19)$$

where the \vec{Y}_{rand} vector implies a random search engine chosen from the predetermined demographics. This is the core principle of EWOA, and an effective optimal path selection process is elaborated below. Clustering-based EWOA begins with a set of solutions chosen randomly for every VZ. The identification address of a specific group of CHs is referenced in each solution. At each cycle, the search agents update their places after either a random

selection search agent or the optimal solution acquired previously. The cost of the subsequent function is then minimized after the solutions have been evaluated:

$$cost = \alpha W_1 + \beta W_2 + \gamma W_3 \quad (20)$$

$$W_1 = \frac{\sum_{i=1}^{SG} E(n_i)}{\sum_{j=1}^K E_{(C,H(p,j))}} \quad (21)$$

$$W_2 = \sum_{j=1}^K \frac{\sum_{i=1}^{NC_{p,j}} dis_{(n_i,CH_{p,j})}}{NC_{p,j}} + \frac{\sum_{j=1}^K dis_{(CH_{p,j},BS)}}{K} \quad (22)$$

$$W_3 = \frac{SG}{\sum_{j=1}^K CM_{S(j,CH_j)}} \quad (23)$$

where the coefficients $\alpha, \beta,$ and γ imply energy, distance, and density parameters. K represents the number of CHs. The function W_1 chooses the collection of CHs with the highest energy level n_i Eq. (21). The function W_2 in Eq. (22) includes the communication cost from CHs to CMs and from CHs to the sink. Additionally, Eq. (23) processes the vehicle density and selects the CHs covering most nodes. According to the following process, the best optimal solution is found in the VANETs to achieve effective performance in high-speed communication.

Division phase: Separate the sensing area into four VZ. Establish the nodes as SG. Initialization phase: Generate W random search agent vectors (sets of CHs' IDs). Create values for $\overline{C}_1, \overline{C}_2, a,$ and M_{axitr} .

Evaluation phase: Estimate the search agents using Eq. (20). Determine the most effective search agent (set of CHs) to serve as the ideal agent.

Updating phase: Adjust the parameters. $\overline{C}_1, \overline{C}_2, a, r_1, l,$ and p . Eqs. (17), (18), and (19) should be used to exploit and explore the search agents based on the values of \overline{C}_2 and p . Limit the range of the search agent values in accordance with the IDs of the CHs. Repeat steps 3 and 4 until the maximum number of repetitions is achieved, or the termination condition is met. Continue using steps 2 and 5 until all the VZ's optimal solutions are identified.

5. Performance analyses

This section compares the performance of the HGFA-VANETs [20] and MOFO-VANETs [21] methods with the composed HOIPS-VANETs. the comparison finds based on the performance calculations. The parameters considered in the research are energy efficiency, packet delivery ratio,

Table 2. Simulation parameters

| Parameters | Values |
|----------------------------|---------------|
| Simulator used | NS2.34 |
| Mobility Model | SUMO |
| Time | 300 ms |
| Map Layout Area | 2000m*2000m |
| No of Vehicles | 1000 Vehicles |
| MAC Layer | IEEE 802.11p |
| Packet Transmission Rate | 1packet/ms |
| Vehicle Transmission Range | 300m |
| Minimum Vehicle Speed | 30 Km/h |
| Queue Type | DropTail |
| Transmission Power | 0.500 Joules |
| Receiving Power | 0.050 Joules |
| Data Packet Size | 512 tes |

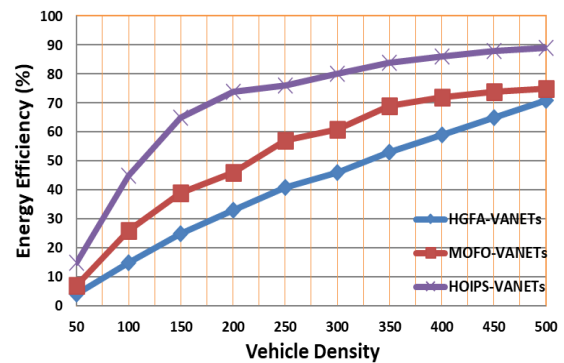


Figure. 4 Energy efficiency calculation

routing overhead, latency, packet loss, throughput, energy consumption, and network lifetime. The input parameters which are considered for the process of simulation are shown in Table 2.

5.1 Energy efficiency calculation

Fig. 4 represents the graphical illustration of energy efficiency calculation. It shows that the HOIPS-VANETs achieve better efficiency when compared with the HGFA-VANETs [20] and MOFO-VANETs [21]. The drawback HOIPS-VANETs is introduced which provide effective initial path selection and clustering based optimal solution finding.

5.2 Packet delivery ratio calculation:

Fig. 5 shows that the HOIPS-VANETs achieve a better packet delivery ratio when compared with the HGFA-VANETs [20] and MOFO-VANETs [21]. A result of those causes the packet delivery ratio attained by the HOIPS-VANETs is higher than that of the earlier methods.

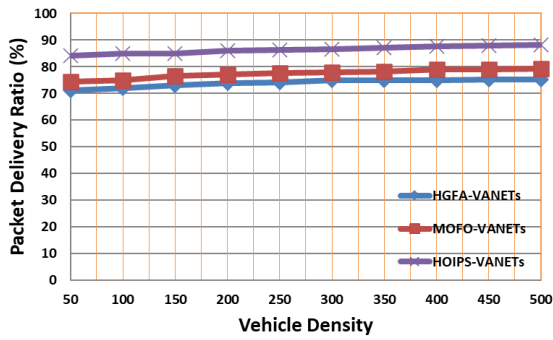


Figure. 5 Packet delivery ratio calculation

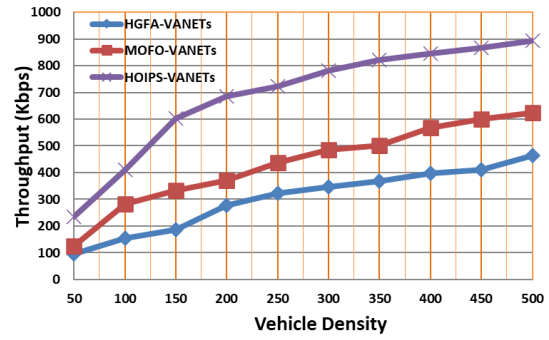


Figure. 8 Packet loss calculation

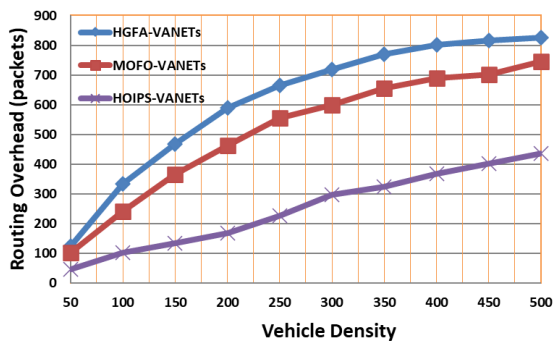


Figure. 6 Routing overhead calculation

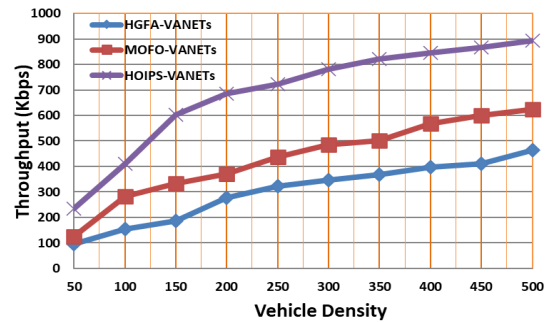


Figure. 9 Throughput calculation

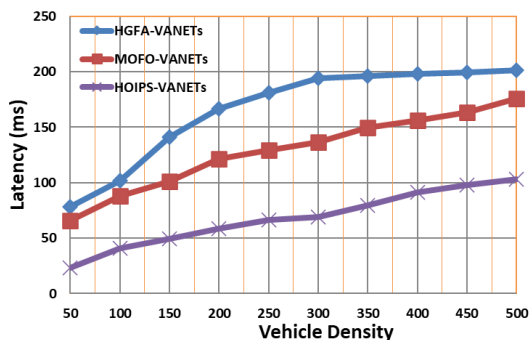


Figure. 7 Latency calculation

5.3 Routing overhead calculation

Fig. 6 shows that the HOIPS-VANETs produced low routing overhead compared to the HGFA-VANETs [20] and MOFO-VANETs [21]. The effective optimization during communication greatly reduces the production of forward packets and decrease of the routing overhead in the HOIPS-VANETs networks compared with the earlier approaches.

5.4 Latency calculation

Fig. 7 shows that the HOIPS-VANETs produced low latency compared to the HGFA-VANETs and MOFO-VANETs. The latency generated by the HOIPS-VANETs approach is lower than the other.

Using the ACO and EWOA algorithms, the overhead produced by the network is also lower, which helps to achieve lower latency during data transmission in high-speed networks.

5.5 Packet loss calculation

Fig. 8 shows that the HOIPS-VANETs produced low packet loss compared to the HGFA-VANETs [21] and MOFO-VANETs [21]. The HOIPS-VANETs cleverly concentrate on clustering effective hybrid optimization for VANETs. The possibility for data loss is extremely minimized even in a densely populated urban environment.

5.6 Throughput calculation

Fig. 9 shows that the HOIPS-VANETs produced higher throughput when compared with the HGFA-VANETs [20] and MOFO-VANETs [21]. The network's fundamental needs to attain maximum throughput at the time of data transmission by using ACO and EWOA algorithms. The parameters are highly reduced which reflects in the achievement of high-speed data transfer.

7.7 Energy consumption calculation

Fig. 10 shows that the HOIPS-VANETs achieve lower energy consumption when compared with the HGFA-VANETs [20] and MOFO-VANETs [21].

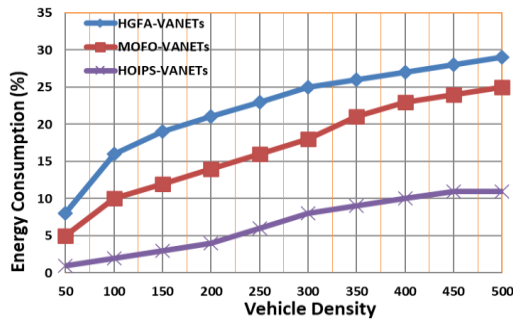


Figure. 10 Energy consumption calculation

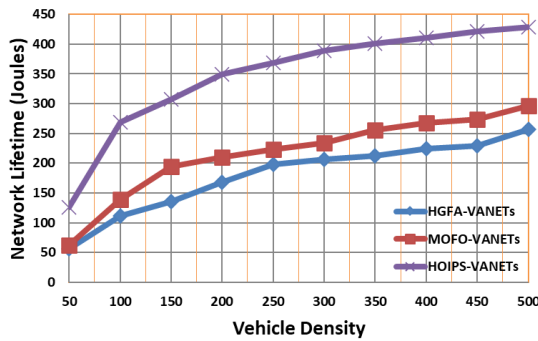


Figure. 11 Network lifetime calculation

The HOIPS-VANETs ingeniously focus on clustering-based effective hybrid optimization for VANETs. The high energy consumption is extremely minimized even in a densely populated urban environment.

5.8 Network lifetime calculation

Fig. 11 shows that the HOIPS-VANETs achieve better network lifetime when compared with HGFA-VANETs [20] and MOFO-VANETs [21]. The consumption of energy for each transmission is moderate due to absence of a proper communication model used in it. The HOIPS-VANETs is focus on effective initial path selection and clustering based optimal solution finding.

6. Results and discussion

This section discusses the measurements of the considered parameters. Table 3 shows the Energy efficiency for the parameter’s energy efficiency, packet delivery ratio and routing overhead.

The energy efficiency completed using the Energy efficiency of the HOIPS-VANETS method is 14% better than MOFO-VANETS, and 18% better than HGFA-VANETS. The packet delivery ratio of the HOIPS-VANETS method is 88.21%, compared with HGFA-VANETS is 75.29% and MOFO-VANETS 79.26%. Hence, the packet delivery ratio

Table 3. The calculation for the energy efficiency, packet delivery ratio and routing overhead parameters

| Vehicle Density | HGFA-VANETS | MOFO-VANETS | HOIPS-VANETS |
|--------------------------------|-------------|-------------|--------------|
| Energy Efficiency | | | |
| 150 | 4.25 | 7.41 | 15.23 |
| 300 | 15.46 | 26.23 | 45.46 |
| 450 | 25.48 | 39.85 | 65.28 |
| 600 | 33.74 | 46.17 | 74.17 |
| 750 | 41.46 | 57.25 | 76.28 |
| 900 | 46.28 | 61.16 | 80.17 |
| 1050 | 53.17 | 69.27 | 84.13 |
| 1200 | 59.76 | 72.16 | 86.25 |
| 1350 | 65.13 | 74.22 | 88.22 |
| 1500 | 71.11 | 75.46 | 89.39 |
| Packet Delivery Ratio | | | |
| 150 | 71.23 | 74.29 | 84.26 |
| 300 | 72.03 | 75.08 | 84.88 |
| 450 | 73.11 | 76.55 | 85.06 |
| 600 | 73.89 | 77.24 | 85.98 |
| 750 | 74.02 | 77.68 | 86.32 |
| 900 | 74.94 | 77.94 | 86.55 |
| 1050 | 75.01 | 78.24 | 87.11 |
| 1200 | 75.09 | 78.99 | 87.69 |
| 1350 | 75.11 | 79.08 | 88.08 |
| 1500 | 75.29 | 79.26 | 88.21 |
| Routing Overhead (PACs) | | | |
| 150 | 125 | 102 | 46 |
| 300 | 333 | 241 | 102 |
| 450 | 468 | 365 | 135 |
| 600 | 589 | 463 | 169 |
| 750 | 666 | 555 | 226 |
| 900 | 719 | 599 | 298 |
| 1050 | 769 | 655 | 324 |
| 1200 | 801 | 689 | 368 |
| 1350 | 816 | 701 | 401 |
| 1500 | 825 | 745 | 435 |

of the HOIPS-VANETS method is 9% better than MOFO-VANETS, and 12% better than HGFA-VANETS. The routing overhead proposed by the HOIPS-VANETS approach is 435 packets. Therefore, the routing overhead of the HOIPS-VANETS approach is 310 packets lower than MOFO-VANETS, 390 packets lower than HGFA-VANETS. Table 4 shows the value calculation for the parameter’s latency, packet loss, and throughput.

In Table 4, the latency proposed via means of the HOIPS-VANETS approach is 102.96 ms, which is for the HGFA-VANETS is 201.49 ms and MOFO-VANETS is 175.68 ms. The latency of the HOIPS-VANETS approach is 70 ms less than MOFO-VANETS, and 95 ms less than HGFA-VANETS. The packet loss proposed via the HOIPS-VANETS approach is 254 packets for the HGFA-VANETS is 568 packets and MOFO-VANETS is 514 packets.

Table 4. The calculation for the latency, packet loss, and throughput parameters

| Vehicle Density | HGFA-VANETs | MOFO-VANETs | HOIPS-VANETs |
|---------------------------|-------------|-------------|--------------|
| Energy Efficiency | | | |
| 150 | 78.12 | 65.79 | 23.28 |
| 300 | 102.09 | 88.26 | 41.08 |
| 450 | 141.06 | 101.08 | 49.67 |
| 600 | 166.87 | 121.44 | 58.64 |
| 750 | 181.23 | 129.33 | 66.39 |
| 900 | 194.37 | 136.55 | 69.35 |
| 1050 | 196.34 | 149.87 | 79.64 |
| 1200 | 198.46 | 156.38 | 91.06 |
| 1350 | 199.48 | 163.44 | 98.22 |
| 1500 | 201.49 | 175.68 | 102.96 |
| Packet Loss (PACs) | | | |
| 150 | 96 | 81 | 39 |
| 300 | 355 | 265 | 68 |
| 450 | 469 | 336 | 126 |
| 600 | 498 | 376 | 156 |
| 750 | 526 | 401 | 186 |
| 900 | 539 | 435 | 201 |
| 1050 | 546 | 476 | 223 |
| 1200 | 550 | 498 | 236 |
| 1350 | 561 | 510 | 241 |
| 1500 | 568 | 514 | 254 |
| Throughput (Kbps) | | | |
| 150 | 96.17 | 124.78 | 235.19 |
| 300 | 155.46 | 281.09 | 411.09 |
| 450 | 187.26 | 332.69 | 603.46 |
| 600 | 277.46 | 369.47 | 685.04 |
| 750 | 321.46 | 436.98 | 723.46 |
| 900 | 346.26 | 486.34 | 780.31 |
| 1050 | 368.94 | 501.36 | 821.56 |
| 1200 | 398.34 | 568.19 | 846.07 |
| 1350 | 409.64 | 601.23 | 865.79 |
| 1500 | 465.17 | 625.17 | 894.77 |

Therefore, the packet loss of the HOIPS-VANETS approach is 250 packets less than MOFO-VANETS, and 310 packets less than HGFA-VANETS. The throughput calculated for the HOIPS-VANETS technique is 894.77 Kbps for the HGFA-VANETS is 465.17 Kbps and MOFO-VANETS is 625.17 Kbps. Therefore, the throughput of the HOIPS-VANETS approach is 260 Kbps better than MOFO-VANETS, 430 Kbps better than HGFA-VANETS. Table 5 shows the value calculation for the energy consumption and network lifetime.

In Table 5, the energy consumption proposed via the HOIPS-VANETS is 524%, which for the HGFA-VANETS is 856 % and MOFO-VANETS is 725 %. Therefore, the energy consumption of the HOIPS-VANETS is 200% less than MOFO-VANETS, and 230% less than HGFA-VANETS. The network

Table 5. The calculation for the energy consumption and network lifetime parameters

| Vehicle Density | HGFA-VANETs | MOFO-VANETs | HOIPS-VANETs |
|----------------------------------|-------------|-------------|--------------|
| Energy Consumption | | | |
| 150 | 8.28 | 5.15 | 1.63 |
| 300 | 16.11 | 10.26 | 2.17 |
| 450 | 19.89 | 12.28 | 3.05 |
| 600 | 21.16 | 14.16 | 4.29 |
| 750 | 23.28 | 16.28 | 4.12 |
| 900 | 25.27 | 18.17 | 8.09 |
| 1050 | 26.11 | 21.36 | 8.46 |
| 1200 | 27.92 | 23.22 | 10.17 |
| 1350 | 28.94 | 24.04 | 10.16 |
| 1500 | 29.28 | 25.26 | 11.23 |
| Network Lifetime (Joules) | | | |
| 150 | 56.58 | 61.79 | 125.78 |
| 300 | 111.03 | 139.64 | 268.31 |
| 450 | 135.09 | 194.16 | 306.89 |
| 600 | 168.49 | 209.38 | 349.16 |
| 750 | 198.16 | 222.68 | 368.17 |
| 900 | 206.38 | 233.67 | 389.16 |
| 1050 | 212.06 | 255.39 | 401.28 |
| 1200 | 224.13 | 268.16 | 411.08 |
| 1350 | 229.37 | 274.19 | 421.04 |
| 1500 | 256.25 | 296.28 | 428.19 |

lifetime completed using the HOIPS-VANETS is 542 Joules. The HGFA-VANETS is 154 Joules, MOFO-VANETS is 256 Joules. The Network Lifetime of the HOIPS-VANETS is 190 Joules better than previous strategies.

7. Conclusion

This hybrid optimization concept identifies the shortest path from the source to the destination, reflecting the reduced energy consumption, delay, routing overhead, and packet loss in the network. The algorithms experienced in this research are ACO and EWOA, where the ACO algorithm identifies the initial path towards the destination from the source, and the highly effective best solution according to the vehicle mobility is found with the help of the EWOA algorithm. The implementation is performed in NS2 and the results of the HOIPS-VANETS are compared with the HGFA-VANETS and MOFO-VANETS. The results are observed that the HOIPS-VANETS achieve better energy efficiency, better packet delivery ratio, lower routing overhead, 20 ms to 95 ms less latency, less packet loss, better throughput, lower energy consumption and 100 joules to 200 joules high network lifetime when compared with the earlier approaches. In the future direction to increase the density of the network clustering will get included in VANETS.

Conflicts of interest

Conflicts of Interest: The authors declare no conflict of interest

Author contributions

Conceptualization, F. Al-dolaimy, Rabei Raad Ali and Salama A Mostafa; methodology, Noor Nabeel, Mohammed Ahmed Jubair; software, Mohammed Ahmed Jubair, and Wisam Subhi Al-Dayyeni; validation, Fatima Hashim Abbas, Hussein Muhi Hariz and Rabei Raad Ali; formal analysis, Noor Nabeel, Wisam Subhi Al-Dayyeni, and Mohammed Ahmed Jubair; investigation, Noor Nabeel and Wisam Subhi Al-Dayyeni; resources, F. Al-dolaimy, Fatima Hashim Abbas, Hussein Muhi Hariz, Salama A Mostafa and Mohammed Ahmed Jubair; writing—original draft preparation, F. Al-dolaimy; writing—review and editing, Rabei Raad Ali and Salama A Mostafa; supervision, Rabei Raad Ali, Salama A Mostafa and Mohammed Ahmed Jubair; project administration, Fatima Hashim Abbas. All authors read and approved the final manuscript.

References

- [1] C. Xu, Z. Xiong, X. Kong, G. Zhao and S. Yu, "A Packet Reception Probability-Based Reliable Routing Protocol for 3D VANET", *IEEE Wireless Communications Letters*, Vol. 9, No. 4, pp. 495-498, April 2020.
- [2] A. F. M. S. Shah, M. A. Karabulut, H. Ilhan, and U. Tureli, "Performance Optimization of Cluster-Based MAC Protocol for VANETs", *IEEE Access*, Vol. 8, pp. 167731-167738, 2020.
- [3] A. Feroz, A. Mehmood, H. Maryam, S. Zeadally, C. Maple, and M. A. Shah, "Vehicle-Life Interaction in Fog-Enabled Smart Connected and Autonomous Vehicles", *IEEE Access*, Vol. 9, pp. 7402-7420, 2021.
- [4] M. A. Hossain, R. M. Noor, K. L. A. Yau, S. R., M. R. A. Z. Abar, I. Ahmedy, and M. R. Jabbarpour, "Multi-objective Harris hawks optimization algorithm based 2-Hop routing algorithm for CR-VANET", *IEEE Access*, Vol. 9, pp. 58230-58242, 2021.
- [5] F. Yang, J. Han, X. Ding, Z. Wei, and X. Bi, "Spectral Efficiency Optimization and Interference Management for Multi-Hop D2D Communications in VANETs", *IEEE Transactions on Vehicular Technology*, Vol. 69, No. 6, pp. 6422-6436, June 2020.
- [6] B. Jiang, S. N. Givigi, and J. A. Delamer, "A MARL Approach for Optimizing Positions of VANET Aerial Base-Stations on a Sparse Highway", *IEEE Access*, Vol. 9, pp. 133989-134004, 2021.
- [7] Z. Khan, S. Fang, A. Koubaa, P. Fan, F. Abbas, and H. Farman, "Street-centric routing scheme using ant colony optimization-based clustering for bus-based vehicular ad-hoc network", *Computers & Electrical Engineering*, Vol. 86, p. 106736. 2020.
- [8] S. Ghosh and I. S. Misra, "Enhanced QoS Performance with Reduced Route Overhead by Ant Colony Optimization Algorithm for VANET", In: *Proc. of 2020 IEEE Applied Signal Processing Conference (ASPCON)*, pp. 237-241, 2020.
- [9] G. A. Ahmed, T. R. Sheltami, A. S. Mahmoud, M. Imran and M. Shoaib, "A Novel Collaborative IoD-Assisted VANET Approach for Coverage Area Maximization", *IEEE Access*, Vol. 9, pp. 61211-61223, 2021.
- [10] H. B. Salau, A. J. Onumanyi, A. M. A. Mahfouz, A. O. Adejo, and M. B. M. Azu, "New Discrete Cuckoo Search Optimization Algorithms for Effective Route Discovery in IoT-Based Vehicular Ad-Hoc Networks", *IEEE Access*, Vol. 8, pp. 145469-145488, 2020.
- [11] R. R. Ali, S. A. Mostafa, H. Mahdin, A. Mustapha, and S. S. Gunasekaran, "Incorporating the Markov Chain model in WBSN for improving patients' remote monitoring systems", In: *Recent Advances on Soft Computing and Data Mining: Proceedings of the Fourth International Conference on Soft Computing and Data Mining (SCDM 2020), Melaka, Malaysia*, pp. 35-46, 2020.
- [12] F. Yang, C. Zhao, X. Ding, and J. Han, "An Analytical Model for Energy Harvest Road Side Units Deployment with Dynamic Service Radius in Vehicular Ad-Hoc Networks", *IEEE Access*, Vol. 8, pp. 122589-122598, 2020.
- [13] Z. Gao, H. C. Wu, S. Cai, and G. Tan, "Tight Approximation Ratios of Two Greedy Algorithms for Optimal RSU Deployment in One-Dimensional VANETs", *IEEE Transactions on Vehicular Technology*, Vol. 70, No. 1, pp. 3-17, 2021.
- [14] J. Liang and M. Ma, "ECF-MRS: An Efficient and Collaborative Framework with Markov-Based Reputation Scheme for IDSs in Vehicular Networks", *IEEE Transactions on Information Forensics and Security*, Vol. 16, pp. 278-290, 2021.
- [15] R. Attia, A. Hassaan, and R. Rizk, "Advanced Greedy Hybrid Bio-Inspired Routing Protocol to Improve IoV", *IEEE Access*, Vol. 9, pp. 131260-131272, 2021.

- [16] C. Ghorai, S. Shakhari, and I. Banerjee, "A SPEA-Based Multimetric Routing Protocol for Intelligent Transportation Systems", *IEEE Transactions on Intelligent Transportation Systems*, Vol. 22, No. 11, pp. 6737-6747, 2021.
- [17] Z. Deng, Z. Cai, and M. Liang, "A Multi-Hop VANETs-Assisted Offloading Strategy in Vehicular Mobile Edge Computing", *IEEE Access*, Vol. 8, pp. 53062-53071, 2020.
- [18] S. Li, F. Wang, J. Gaber, and X. Chang, "Throughput and Energy Efficiency of Cooperative ARQ Strategies for VANETs Based on Hybrid Vehicle Communication Mode", *IEEE Access*, Vol. 8, pp. 114287-114304, 2020.
- [19] L. Zhao, W. Zhao, A. Hawbani, A. Y. A. Dubai, G. Min, A. Y. Zomaya, and C. Gong, "Novel online sequential learning-based adaptive routing for edge software-defined vehicular networks", *IEEE Transactions on Wireless Communications*, Vol. 20, No. 5, pp. 2991-3004, 2020.
- [20] G. D. Singh, M. Prateek, S. Kumar, M. Verma, D. Singh, and H. N. Lee, "Hybrid genetic firefly algorithm-based routing protocol for VANETs", *IEEE Access*, Vol. 10, pp. 9142-9151, 2022.
- [21] Z. Sadreddini, and T. Çavdar, "General resource management via several message criteria in Vehicular Delay Tolerant Networks", In: *Proc. of IEEE 2016 24th Signal Processing and Communication Application Conference (SIU)*, pp. 289-292, 2016.